Kinetic study of the effects of inhibitors on the catalyzed dehydration of HCO3- by copper(II) complexes, [Tp(Ph)]CuX (X- = OH-, N-3(-), NCS-)

ARTICLE *in* INORGANIC CHEMISTRY · JANUARY 2003

Impact Factor: 4.76 · DOI: 10.1021/ic025926h · Source: PubMed

9 AUTHORS, INCLUDING:

Ying-Ji Sun
Dalian University of Technology
26 PUBLICATIONS **241** CITATIONS
SEE PROFILE

Peng Cheng
Nagoya Gakuin University
367 PUBLICATIONS **8,083** CITATIONS
SEE PROFILE

Inorg. Chem. **2003**, *42*, 508–515

Kinetic Study of the Effects of Inhibitors on the Catalyzed Dehydration of HCO_3^- by Copper(II) Complexes [Tp^{Ph}]CuX ($X^- = OH^-$, N_3^-, NCS^-)

Ying-Ji Sun, Lei Z. Zhang, Peng Cheng,* Hua-Kuan Lin, Shi-Ping Yan, Wei Sun, Dai-Zheng Liao, Zong-Hui Jiang, and Pan-Wen Shen

Department of Chemistry, Nankai University, Tianjin 300071, P.R. China

Received August 3, 2002

A series of half-sandwich copper(II) complexes [Tp^{Ph}]CuX ([Tp^{Ph}] = hydrotris(3-phenyl-pyrazolyl)borate; $X^- = OH^-$ (**1**), N_3^- (**2**), NCS^- (**3**)) have been synthesized as models for carbonic anhydrase. The structure of **3** was determined by X-ray diffraction analysis. Crystals of **3** ($C_{37}H_{30}BCuN_9S$) are triclinic, space group $P\bar{1}$ with $a = 11.997(3)$ Å, $b = 12.116(3)$ Å, $c = 13.384(4)$ Å, $\alpha = 81.088(5)°$, $\beta = 79.289(6)°$, $\gamma = 68.668(5)°$, $V = 1772.4(8)$ Å^3, and $Z = 2$. The dehydration kinetic measurements of HCO_3^- are performed by the stopped-flow techniques at pH < 7.9. The apparent dehydration rate constant k^d_{obs} varies linearly with total Cu(II) concentration, and the catalytic activity of the model complexes decreases in the order **1** > **2** > **3**. The catalytic activity decreases with increasing pH indicating that the aqua model complex must be the reactive catalytic species in the catalyzed dehydration reaction and the rate-determining step is the substitution of the labile water molecule by HCO_3^-. The k^d_{obs} values increase with increasing reaction temperature, and the apparent activation energies of the model complexes with inhibitors are remarkably higher than that of the complex with no inhibitors, this being the origin of inhibition. The large negative entropy of activation also indicates an associative mode of activation in the rate-determining step. The inhibition ability of the inhibitor NCS^- is stronger than that of the inhibitor N_3^-, which can be rationalized by the decrease in effective atomic charges of the Cu(II) ions as revealed by the theoretical calculations.

1. Introduction

In modern bioinorganic chemistry, CO_2 hydration and its mechanism in living systems has been a topic of great interest.[1−3] Carbonic anhydrases (CAs) are a family of zinc enzymes found in animals, plants, and bacteria, with the essential physiological function to catalyze the reversible hydration of carbon CO_2.[4−8] The most widely accepted catalytic cycle for CA is the so-called zinc−hydroxide mechanism, denoted here as mechanism I (see Scheme 1).[9−12] The catalytic activity is characterized by a pK_a value of ca. 7.0, such that hydration of CO_2 is dominant above pH 7, while dehydration of HCO_3^- is observed below pH 7.[13] It has been postulated that this pK_a value represents that of the coordinated water molecule on the Zn(II) ion center. It should be noted that the catalytic activities of CA are greatly inhibited in the presence of inhibitors.[14,15] Most of the strong inhibitors are small inorganic anions (e.g., NCS^-, N_3^-, I^-, NO_2^-), inhibition by which is understandable in light of the

* To whom correspondence should be addressed. E-mail: pcheng@nankai.edu.cn. Fax: +86-22-23502458.

(1) Dodgson, S. J.; Tashian, R. E.; Gros, G.; Carter, N. D. *The Carbonic Anhydrase: Cellular Physiology and Molecular Genetics*; Plenum Press: New York, 1991.
(2) Botre, F.; Gros, G.; Storey, B. T. *Carbonic Anhydrase*; VCH: Weinheim, Germany, 1991.
(3) Christianson, D. W. *Adv. Protein Chem.* **1991**, *41*, 281.
(4) Christianson, D. W.; Fierke, C. A. *Acc. Chem. Res.* **1996**, *29*, 331.
(5) (a) Coleman, J. E. *J. Biol. Chem.* **1967**, *242*, 5212. (b) Coleman, J. E. In *Zinc Enzyme*; Bertini, I., Luchinat, C., Maret, W., Zeppezauer, M., Eds.; Birkhäuser: Boston, 1986.
(6) (a) Lindskog, S. In *Zinc Enzyme*; Spiro, T. G., Ed.; Wiley: New York, 1983. (b) Silverman, D. N.; Lindskog, S. *Acc. Chem. Res.* **1988**, *21*, 30.
(7) Sly, W. S.; Hu, P. Y. *Annu. Rev. Biochem.* **1995**, *64*, 375.
(8) Schindler, S.; Hubbard, C. D.; van Eldik, R. *Chem. Soc. Rev.* **1998**, *27*, 387.
(9) (a) Bertini, I.; Mangani, S.; Pierattelli, R. *International Conference on Carbon Dioxide Utilization: Lectures and Posters*; University of Bari: Bari, Italy, 1993. (b) Bertini, I.; Luchinat, C. In *Bioinorganic Chemistry*; Bertini, I., Gray, H. B., Lippard, S. J., Valentine, J. S., Eds.; University Science Books: Sausalito, CA, 1994.
(10) (a) Eriksson, A. E.; Jones, T. A.; Liljas, A. *Proteins: Struct., Funct., Genet.* **1988**, *4*, 274. (b) Xue, Y.; Vidgren, J.; Svensson, L. A.; Liljias, A.; Jonsson, B.-H.; Linskog, S. *Proteins: Struct., Funct., Genet.* **1993**, *15*, 80.
(11) Nair, S. K.; Christianson, D. *J. Am. Chem. Soc.* **1991**, *113*, 9455.
(12) Merz, K.; Murcko, M. A.; Kollman, P. A. *J. Am. Chem. Soc.* **1991**, *113*, 4484.
(13) Bertini, I.; Luchinat, C.; Scozzafava, A. *Struct. Bonding (Berlin)* **1982**, *48*, 45.
(14) Liang, J.; Lipscomb, W. N. *Biochemistry* **1989**, *28*, 9724.

10.1021/ic025926h CCC: $25.00
Published on Web 12/21/2002

Scheme 1

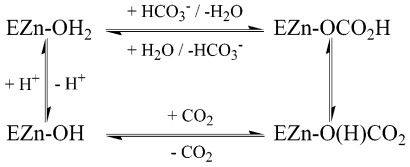

known enzyme−substrate complex formed between CA and HCO_3^-.[16] Despite the numerous papers in recent years focusing on the kinetic study of new model complexes for CA,[17−19] studies concerning the role of inhibitors during the dehydration process of HCO_3^- are relatively few.[20,21] By performing kinetic measurements on a series of half-sandwich CA model complexes, it is our intention in this present contribution to (1) elucidate the origin of inhibition by a detailed study of the effects of inhibitors on the dehydration reaction of HCO_3^- and (2) rationalize the variations in inhibition ability between two different inhibitors.

Trofimenko's hydrotris(pyrazolyl)borate ligand system [Tp^R] has been applied to synthesize the model complexes (Figure 1).[22,23] The trigonally capping Tp^R has the advantage over other ligand systems in mimicking the coordination environment of CA made by three histidyl residues. Because zinc(II) complexes are spectroscopically inert, we have therefore synthesized a series of half-sandwich copper(II) complexes [Tp^{Ph}]CuX ([Tp^{Ph}] = hydrotris(3-phenylpyrazolyl)borate; $X^- = OH^-$ (**1**), N_3^- (**2**), NCS^- (**3**)), which are very suitable for spectroscopic analysis by using stopped-flow techniques. The paper is organized as follows: the experimental preparations of the model complexes, X-ray crystallographic analysis, kinetic measurements, and computational methodology are described in the second section. The detailed data analyses and explanations of the effects of inhibitors on the dehydration of HCO_3^- catalyzed by the model complexes are presented in the third section, in the order of the following four aspects: concentration of the model complexes, pH value, free inhibitors, and temperature. In particular, the inhibition ability between the two different inhibitors N_3^- and NCS^- is discussed. Finally, the effects of inhibitors on the dehydration reaction are summarized in the fourth section.

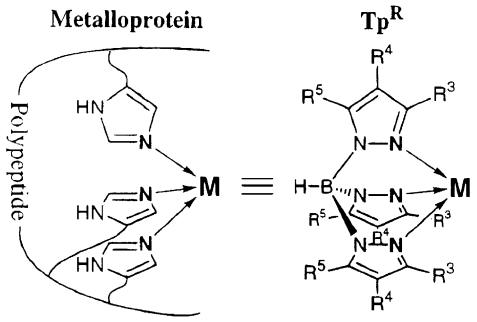

Figure 1. Concept of the application of Tp^R to biological inorganic chemistry.

2. Experimental Section

Starting Materials. All the starting chemicals used in this work were of analytical reagent grade and used without further purification, unless otherwise stated. Hydrotris(3-phenyl-pyrazolyl)borate (Tp^{Ph}) was synthesized according to the literature method,[24] and the purity was confirmed by IR, MS-FAB, and elemental analysis. The indicator bromocresol purple (Sigma) and the biological buffer Tris (tris(hydroxymethyl)aminomethane, Sigma) were purchased and used as received. All solutions were prepared using double distilled water that was boiled for more than 2 h prior to use to remove the dissolved CO_2. The concentrations of the indicator, Tris, and $NaClO_4$ were kept at 2.5×10^{-4}, 7.0×10^{-2}, and 7.5×10^{-2} M, respectively.

Physical Measurements. Elemental analyses for C, H, and N were carried out on a Perkin-Elmer analyzer at the Institute of Elemento-Organic Chemistry, Nankai University. Infrared spectra on KBr pellets were recorded on a Shimadzu IR-408 spectrophotometer in the range 4000−600 cm^{-1}. UV−vis spectra in methanol were recorded on a Shimadzu UV-2101 spectrophotometer in the range 1000−200 nm. The X-band ESR spectra of polycrystalline powder were collected on a Bruker ER 200 D-SRC ESR spectrometer at both room temperature and 77 K. Mass spectra were obtained at the Central Laboratory of Nankai University on VG ZAB-HS spectrometer.

Synthesis of Complex 1: [Tp^{Ph}]CuOH. $Cu(ClO_4)_2 \cdot 6H_2O$ (74.1 mg, 0.2 mmol) in 5 mL of methanol was added dropwise to 10 mL of methanol containing K[Tp^{Ph}] (95.9 mg, 0.2 mmol). The mixture was stirred at room temperature for 2 h. Then, the pH value of the mixture was adjusted to ca. 8 by adding KOH (1 M) and stirred for another 10 h. Blue microcrystals for **1** were obtained and recrystallized from methanol (96.0 mg, yield 92%). IR (KBr pellet): 2420 (B−H), 3605 (O−H) cm^{-1}. Anal. Calcd for $C_{27}H_{23}$-

(15) (a) Cappalonga Bunn, A. M.; Alexander, R. S.; Christianson, D. W. *J. Am. Chem. Soc.* **1994**, *116*, 5063. (b) Kim, C.-Y.; Chang, J. S.; Doyon, J. B.; Baird, T. T., Jr.; Fierke, C. A.; Jain, A.; Christianson, D. W. *J. Am. Chem. Soc.* **2000**, *112*, 12125. (c) Kim, C.-Y.; Chandra, P. P.; Jain, A.; Christianson, D. W. *J. Am. Chem. Soc.* **2001**, *123*, 9620.

(16) Koike, T.; Kimura, E.; Nakamura, I.; Hashimoto, Y.; Shiro, M. *J. Am. Soc. Chem.* **1992**, *114*, 7338.

(17) (a) Zhang, X.; van Eldik, R.; Koike, T.; Kimura, E. *Inorg. Chem.* **1993**, *32*, 5749. (b) Zhang, X.; van Eldik, R. *Inorg. Chem.* **1995**, *34*, 5606. (c) Schrodt, A.; Neubrand, A.; van Eldik, R. *Inorg. Chem.* **1997**, *36*, 4579. (d) Hartmann, M.; Clark, T.; van Eldik, R. *J. Am. Chem. Soc.* **1997**, *119*, 7843. (e) Mao, Z.-W.; Liehr, G.; van Eldik, R. *J. Am. Chem. Soc.* **2000**, *122*, 4839. (f) Mao, Z.-W.; Liehr, G.; van Eldik, R. *J. Chem. Soc., Dalton Trans.* **2001**, 1593.

(18) (a) Kimura, E.; Koike, K.; Shionoya, M. *Struct. Bonding (Berlin)* **1997**, *89*, 1. (b) Kimura, E. *Prog. Inorg. Chem.* **1994**, *11*, 443. (c) Kimura, E.; Shiota, T.; Koike, T.; Shiro, M.; Kodama. M. *J. Am. Chem. Soc.* **1990**, *112*, 5805. (d) Koike, T.; Kimura, E. *J. Am. Chem. Soc.* **1991**, *113*, 8935. (e) Koike, T.; Takamura, M.; Kimura, E. *J. Am. Chem. Soc.* **1994**, *116*, 8443.

(19) (a) Alsfasser, R.; Powell, A. K.; Vahrenkamp, H. *Angew. Chem., Int. Ed. Engl.* **1990**, *29*, 898. (b) Looney, A.; Parkin, G.; Alsfasser, R.; Ruf, M.; Vahrenkamp, H. *Angew. Chem., Int. Ed. Engl.* **1992**, *31*, 92. (c) Alsfasser, R.; Powell, A. K.; Trofimenko, S.; Vahrenkamp, H. *Chem. Ber.* **1993**, *126*, 685. (d) Alsfasser, R.; Trofimenko, S.; Looney, A.; Parkin, G.; Vahrenkamp, H. *Inorg. Chem.* **1991**, *30*, 4098.

(20) (a) Alzuet, G.; Casanova, J.; Borrás, J.; García-Granda, S.; Gutiérrez-Rodríguez, A.; Supuran, C. T. *Inorg. Chim. Acta* **1998**, *273*, 334. (b) Alzuet, G.; Ferrer-Llusar, S.; Borrás, J.; Server-Carrió, J.; Martínez-Máñez, R. *J. Inorg. Biochem.* **1999**, *75*, 189.

(21) Supuran, C. T.; Scozzafava, A.; Mincione, F.; Menabuoni, L.; Briganti, F.; Mincione, G.; Jitianu, M. *Eur. J. Med. Chem.* **1999**, *34*, 585.

(22) (a) Trofimenko, S. *J. Am. Chem. Soc.* **1966**, *88*, 1842. (b) Trofimenko, S. *Chem. Rev.* **1993**, *93*, 943.

(23) Hikichi, S.; Akita, M.; Moro-oka, Y. *Coord. Chem. Rev.* **2000**, *198*, 61.

(24) Eichhorn, D. E.; Armstrong, W. H. *Inorg. Chem.* **1990**, *29*, 3607.

$BCuN_6O$: C, 62.17; H, 4.41; N, 16.10. Found: C, 62.14; H, 4.44; N, 16.08.

Synthesis of Complex 2: [Tp^{Ph}]CuN$_3$. $Cu(ClO_4)_2 \cdot 6H_2O$ (74.1 mg, 0.2 mmol) in 5 mL of methanol was added dropwise to 10 mL of methanol containing K[Tp^{Ph}] (95.9 mg, 0.2 mmol). The mixture was stirred at room temperature for 10 h. Then, NaN_3 (39.1 mg, 0.6 mml) dissolved in the minimum water was added to the mixture and stirred for another 10 h. Green microcrystals for **2** were obtained and recrystallized from methanol (78.7 mg, yield 72%). IR (KBr pellet): 2450 (B—H), 2095 (N≡N) cm^{-1}. Anal. Calcd for $C_{27}H_{22}BCuN_9$: C, 59.33; H, 4.02; N, 23.05. Found: C, 58.85; H, 4.05; N, 22.97.

Synthesis of Complex 3: [Tp^{Ph}]Cu(NCS)(Hpz^{Ph}). The same procedure used for **2** was employed. From $Cu(ClO_4)_2 \cdot 6H_2O$ (74.1 mg, 0.2 mmol), K[Tp^{ph}] (95.9 mg, 0.2 mmol), and KSCN (58.2 mg, 0.6 mmol) was obtained **3**. Green single crystals suitable for X-ray diffraction analysis were obtained from slow evaporation of the filtrate (97.6 mg, yield 69%). IR (KBr pellet): 2450 (B—H), 2075 (C≡N) cm^{-1}. Anal. Calcd for $C_{37}H_{30}BCuN_9S$: C, 62.85; H, 4.24; N, 17.82. Found: C, 62.69; H, 4.28; N, 17.65.

X-ray Crystallographic Analysis for 3. A single crystal of **3** with approximate dimensions of 0.20 × 0.25 × 0.30 mm^3 was mounted on a glass fiber. A full data collection was performed with graphite monochromatized Mo Kα radiation (λ = 0.71073 Å) on a Bruker SMART 1000 diffractometer equipped with a CCD camera. Cell parameters were determined from a least-squares refinement in the range 1.56° < θ < 25.03° at 298(2) K. The intensities of the ±*hkl* reflections were measured up to θ_{max} = 25.03° using an $\omega-2\theta$ scan technique. The absorption correction was performed empirically.[25] The structure was solved by direct methods using SHELXS-97[26] and refined by the full-matrix least-squares method on F^2 using SHELXL-97.[27] All non-hydrogen atoms were refined anisotropically, while hydrogen atoms were set in calculated positions and treated as riding atoms with a common fixed isotropic thermal parameter. The final cycle of the refinement was based on 4048 observed reflections to give R = 0.0562 and R_w = 0.1438. Further data of the X-ray structure analysis are given in Table 1. Selected bond lengths and angles are listed in Table 2.

Dehydration Kinetics of HCO_3^-. All kinetic measurements in 70% ethanol/H_2O (vol/vol) mixed solution were made with a Union Giken RA-401 stopped-flow spectrophotometer equipped with a Union Giken RA-451 rapid-scan attachment in order to determine the change in absorption of the reaction mixture directly after mixing under a certain light wavelength. Temperature was maintained by using a Union Giken RA-454 superthermostat, and temperature accuracy is within 0.1 K. The pH values in this work were all directly measured by means of a Beckman Φ71 pH meter. The ionic strength of all test solutions was adjusted to 0.11 M with the aid of $NaClO_4$ for the dehydration reaction. HCO_3^- solutions (7.5 × 10^{-3} M) were freshly prepared from $NaHCO_3$ and used within 10 h. The most appropriate pH value and light wavelength to study the reaction for this buffer—indicator pair (Tris with bromocresol purple) are ca. 7.0 and 595 nm, respectively, which are revealed by UV—vis absorption spectra. Therefore, the reaction is monitored at 595 nm with a tungsten lamp as the light source.[8] The apparent first-order dehydration rate constants (k^d_{obs}'s) were obtained with at least three half-lives and represent the average of the best three runs. Reproducibility of the values of k^d_{obs} was better than ±5%.

Table 1. Crystallographic Parameters of Complex [Tp^{Ph}]Cu(NCS)(Hpz^{Ph}), **3**[a]

formula	$C_{37}H_{30}BCuN_9S$
fw	707.11
T, K	298(2)
cryst syst	triclinic
space group	$P\bar{1}$
unit cell dimens	
a, Å	11.997(3)
b, Å	12.116(3)
c, Å	13.384(4)
α, deg	81.088(5)
β, deg	79.289(6)
γ, deg	68.668(5)
V, Å^3	1772.4(8)
Z	2
ρ(calcd), g/cm^3	1.325
λ(Mo Kα), Å	0.71073
μ(Mo Kα), mm^{-1}	0.715
GOF	0.987
no. unique reflns	6236
no. obsd reflns ($I > 2\sigma(I)$)	4048
R	0.0562
R_w	0.1438

[a] $R = \sum||F_o| - |F_c||/\sum|F_o|$; $R_w = (\sum w(F_o^2 - F_c^2)^2/\sum(F_o^2)^2)^{1/2}$; $w = 1/[\sigma^2(F_o^2) + (0.0975P)^2 + 0.0000P]$, where $P = (F_o^2 + 2F_c^2)/3$.

Table 2. Selected Bond Lengths [Å] and Angles (deg) of Complex [Tp^{Ph}]Cu(NCS)(Hpz^{Ph}), **3**

Cu(1)—N(8)	2.029(3)
Cu(1)—N(3)	2.044(3)
Cu(1)—N(1)	2.020(3)
Cu(1)—N(5)	2.229(3)
Cu(1)—N(7)	1.933(4)
S(1)—C(10)	1.608(6)
N(7)—C(10)	1.132(6)
N(8)—Cu(1)—N(3)	173.66(13)
N(8)—Cu(1)—N(1)	89.15(13)
N(8)—Cu(1)—N(5)	88.23(13)
N(8)—Cu(1)—N(7)	90.71(15)
N(3)—Cu(1)—N(1)	85.61(13)
N(3)—Cu(1)—N(5)	88.48(12)
N(3)—Cu(1)—N(7)	95.58(15)
N(7)—Cu(1)—N(1)	152.59(17)
N(7)—Cu(1)—N(5)	114.40(17)
N(1)—Cu(1)—N(5)	92.99(13)
C(10)—N(7)—Cu(1)	156.7(5)
N(7)—C(10)—S(1)	175.4(5)

Computational Methodology. During the dehydration process of HCO_3^-, the nucleophilic attack of the free HCO_3^- on the Cu(II) ion of the model complex is affected by the effective atomic charge of the Cu(II) ion. To obtain information on the variations in the effective atomic charge of the Cu(II) ion by coordinating different inhibitors (N_3^-/NCS^-), we have carried out theoretical calculations of **2** and **3** at the UHF level, using a lanl2dz basis set for the Cu atoms and the corresponding basis set for each of the other atoms. These basis sets consisted of the Los Alamos effective core potential (ECP) for Cu with the outermost core orbitals included in the valence description[28] and the 6-31G** basis functions for H, B, C, N, O, and S.[29] Considering that the Mulliken population analysis is very dependent on the basis set used, we have performed a natural bond order (NBO) population analysis, which works better in these cases. The geometric parameters employed in the calculations were

(25) Sheldrick, G. M. *SADABS*; University of Göttingen: Göttingen, Germany, 1996.
(26) Sheldrick, G. M. *SHELXS-97*; University of Göttingen: Göttingen, Germany, 1997.
(27) Sheldrick, G. M. *SHELXL-97*; University of Göttingen: Göttingen, Germany, 1997.
(28) (a) Hay, P. J.; Wadt, W. R. *J. Chem. Phys.* **1985**, *82*, 270. (b) Wadt, W. R.; Hay, P. J. *J. Chem. Phys.* **1985**, *82*, 284. (c) Hay, P. J.; Wadt, W. R. *J. Chem. Phys.* **1985**, *82*, 299.
(29) Dunning, T. H., Jr.; Hay, P. J. In *Modern Theoretical Chemistry*; Schaefer, H. F., III, Ed., Plenum: New York, 1976.

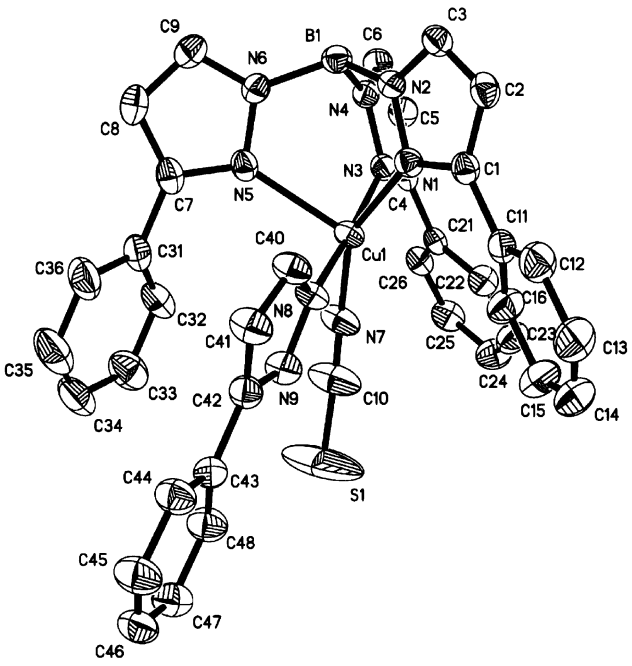

Figure 2. Molecular structure diagram (30% probability) of **3**. Hydrogen atoms are omitted for clarity.

based on the X-ray crystallographic data in this work. All calculations were carried out using the Gaussian-98 package.[30]

3. Results and Discussion

Syntheses and Structural Characterizations of the Model Complexes. Because the active site of CA is of the composition $[His]_3Zn^{II}-OH_2$, where $[His]_3$ refers to three histidyl residues, a rational approach toward obtaining synthetic analogues is to use tridentate ligands in mimicking the protein ligation. Trofimenko's hydrotris(pyrazolyl)borate ligand system [Tp^R], in which three pyrazolyl groups are attached to a common tetrahedral or trigonal pyramidal center, has the advantage over other ligand systems in mimicking the CA coordination environment. To gain a deep insight into the correlation between structure and function, we have analyzed the crystal structure of one model complex by single-crystal X-ray diffraction. The molecular structure diagram of **3** is shown in Figure 2. Despite the ligands Hpz^{Ph} and NCS^-, the complex [Tp^{Ph}]Cu shows a pesudo-C_{3v} symmetry. The coordination geometry about the Cu(II) ion center is best described as trigonal bipyramidal formed by three nitrogen atoms of Tp^{Ph}, one nitrogen atom of N_3^-, and one nitrogen atom of Hpz^{Ph}. N(3)(Tp^{Ph}) and N(8)(Hpz^{Ph}) atoms occupy the axial positions with the N(8)−Cu(1)−N(3) bond angle 173.66(13)°. It should be noted that Hpz^{Ph} is derived from partial decomposition of the ligand Tp^{Ph} during the synthetic procedure. This coordination environment of the Cu(II) ion is quite similar to that of the five-coordinated adduct of the active site of CA as shown in the first section. The average Cu−N(Tp^{Ph}) bond length is 2.10 Å, which is comparable with 2.11 Å in HCA II. The Cu−N(N_3^-) bond length is 1.933 Å.

The powder X-band ESR spectra of **1**−**3** were also recorded at both room temperature and 110 K, and the latter are shown in Figure 3. The ESR spectra remain essentially down to 110 K, without any detectable modification of the relative intensities of the peaks. The spectra of **1** and **2** are rather similar, but different from that of **3**, which may result from the variations in coordination atmospheres of copper(II) ions. It has been considered that the coordination geometry of the Cu(II) ion is tetrahedral for **1** and **2** in the solid-state, while it is trigonal bipyramidal for **3** in the solid-state. The ESR parameters obtained from the spectra are listed in Table 3. All the solid spectra are axial with $g_z > g_x(g_y) > g_e$ indicating a basically $d_{x^2-y^2}$ ground state for the Cu(II) ion, which is consistent with the X-ray crystallographic data.

Dehydration Kinetics of HCO_3^-. As mentioned in the previous section, remarkable changes in absorption at ca. 595 nm were observed when HCO_3^- was added to the reaction mixture, whereas the hydrogen ion concentration was maintained at a constant by means of buffer solutions. The variation of the 595 nm absorption band should relate to the dehydration reaction in this buffer−indicator pair solution.[8] A first-order reaction with respect to the concentration of the Cu(II) complex was observed in all the cases; that is, the dehydration kinetics of HCO_3^- follow the rate law $V^d = k^d_{obs}C_{com}$, where k^d_{obs} is the apparent first-order dehydration rate constant and C_{com} is the total concentration of the complex. The catalytic activity of model complexes is characterized by the pK_a value. The dehydration kinetic measurements of HCO_3^- should be carried out in the case of pH < pK_a to avoid the interference of the reverse hydration reaction especially at higher pH. pH titrations of the model complexes were performed in the pH range 6−8, which established that two species $LCuOH_2^+$ and LCuOH are formed as given in eq 1 (L = ligand).

$$LCuOH_2^+ \rightleftharpoons LCuOH + H^+ \qquad (1)$$

The pK_a values are found to be around 7.9 for the described compounds but are not the same as each other. To understand the effects of inhibitors on the dehydration of HCO_3^-, the apparent dehydration rate constants k^d_{obs} of the model complexes in the absence and presence of inhibitors are measured in the order of four aspects: concentration of the model complexes, pH value, free inhibitors, and temperature.

Concentration of the Model Complexes. Typical kinetic traces observed for different concentrations of the catalyzed dehydration of HCO_3^- by the Cu(II) complexes at pH = 7.014 (≈7.0, the most appropriate pH value to study the

(30) Frisch, M. J.; Trucks, G. W.; Schlegel, H. B.; Scuseria, G. E.; Robb, M. A.; Cheeseman, J. R.; Zakrzewski, V. G.; Montgomery, J. A., Jr.; Stratmann, R. E.; Burant, J. C.; Dapprich, S.; Millam, J. M.; Daniels, A. D.; Kudin, K. N.; Strain, M. C.; Farkas, O.; Tomasi, J.; Barone, V.; Cossi, M.; Cammi, R.; Mennucci, B.; Pomelli, C.; Adamo, C.; Clifford, S.; Ochterski, J.; Petersson, G. A.; Ayala, P. Y.; Cui, Q.; Morokuma, K.; Malick, D. K.; Rabuck, A. D.; Raghavachari, K.; Foresman, J. B.; Cioslowski, J.; Ortiz, J. V.; Stefanov, B. B.; Liu, G.; Liashenko, A.; Piskorz, P.; Komaromi, I.; Gomperts, R.; Martin, R. L.; Fox, D. J.; Keith, T.; Al-Laham, M. A.; Peng, C. Y.; Nanayakkara, A.; Gonzalez, C.; Challacombe, M.; Gill, P. M. W.; Johnson, B. G.; Chen, W.; Wong, M. W.; Andres, J. L.; Head-Gordon, M.; Replogle, E. S.; Pople, J. A. *Gaussian 98*, revision A.9; Gaussian, Inc.: Pittsburgh, PA, 1998.

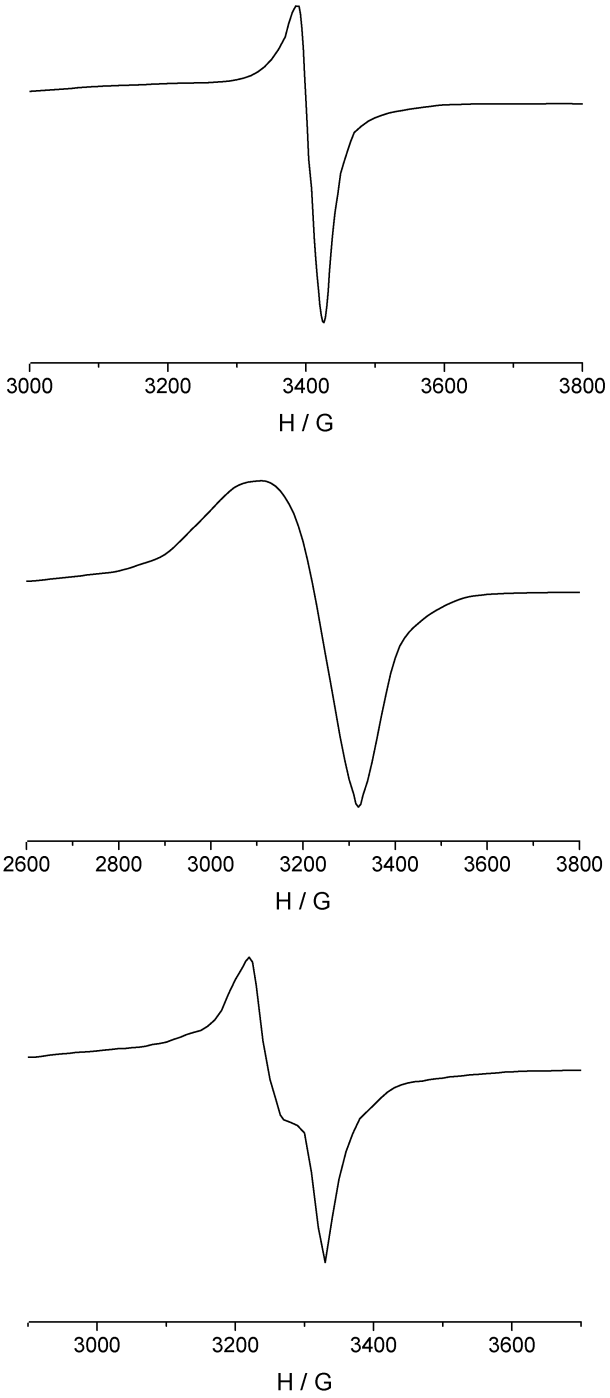

Figure 3. Powder X-band ESR spectra of **1**−**3** at 110 K.

Table 3. ESR Spectra Data of **1**−**3**

complex	g_x(RT)	g_x(LT)	g_y(RT)	g_y(LT)	g_z(RT)	g_z(LT)
1	2.047	2.052	2.055	2.063	2.260	2.259
2	2.099	2.070	2.099	2.070	2.228	2.210
3	2.031	2.034	2.094	2.088	2.126	2.102

reaction as denoted in section 2) are shown by the plot of k^d_{obs} versus [Cu^{2+}] in Figure 4 (Cu^{2+} = copper(II) complex). It is evident that the apparent dehydration rate constant k^d_{obs} varies linearly with total Cu(II) concentration. Hence, a typical catalyst concentration of 1.5×10^{-4} M is selected and used in the following measurements. The catalytic

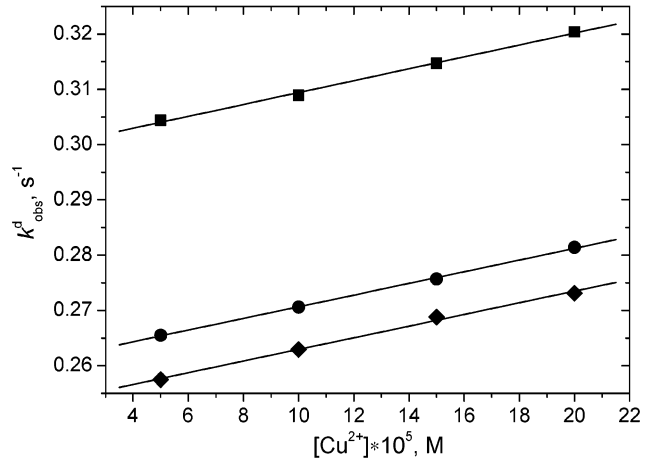

Figure 4. Plot of k^d_{obs} versus [Cu^{2+}] for the dehydration of HCO_3^-. Experimental conditions: pH = 7.014; [$NaHCO_3$] = 7.5×10^{-3} M; ionic strength = 0.11 M; [buffer] = 7.0×10^{-2} M; [indicator] = 2.5×10^{-4} M; temperature = 25.0 °C. Key: (■) **1**; (●) **2**; (◆) **3**.

Scheme 2

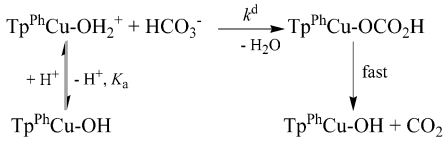

Scheme 3

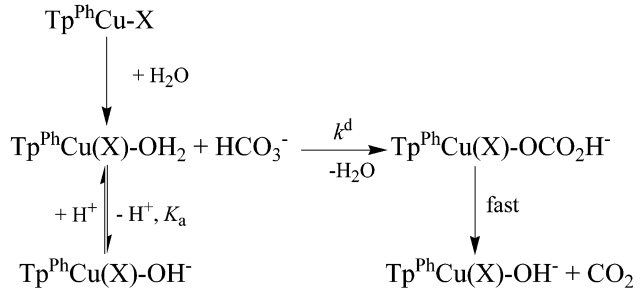

activity of the model complexes decreases in the order **1** > **2** > **3**, which shows that the dehydration process is affected by the Cu(II) complexes with inhibitors. The effect of free Cu(II) ions on the reaction was also checked at the same pH value, but no catalysis was observed. This indicates that the dehydration reactions are indeed catalyzed by the half-sandwich copper(II) complexes.

pH Value. To examine the effects of pH value on the catalytic reactions, the dehydration kinetics of HCO_3^- catalyzed by the model complexes were then studied in the pH range 7.0−7.9 under the same experimental conditions. The pH range was once again restricted by the interference of the hydration reaction of CO_2 at higher pH values. The pH dependence of k^d_{obs} can be accounted for in terms of the mechanisms II and III outlined in Schemes 2 and 3, respectively, which are based on the principle that only the aqua complex can react with HCO_3^- in order to catalyze the dehydration reaction ($X^- = N_3^-/NCS^-$).[31] In these two mechanisms, it is assumed that the produced bicarbonate complex is unstable and rapidly releases CO_2. It is reasonable

(31) Palmer, D. A.; van Eldik, R. *Chem. Rev.* **1983**, *83*, 651.

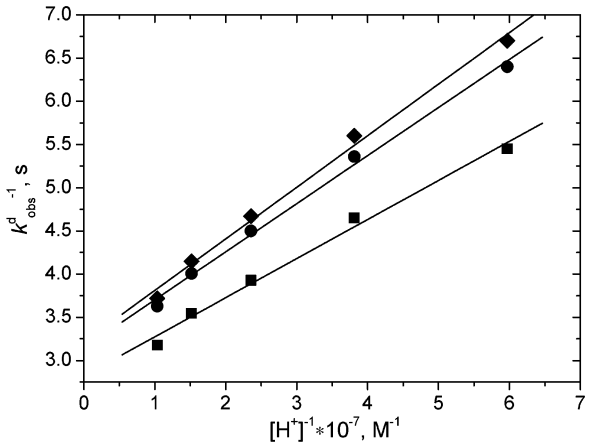

Figure 5. Plot of $k^d_{obs}{}^{-1}$ versus $[H^+]^{-1}$ for the dehydration of HCO_3^-. Experimental conditions: $[NaHCO_3] = 7.5 \times 10^{-3}$ M; $[Cu^{2+}] = 1.5 \times 10^{-4}$ M; ionic strength = 0.11 M; [buffer] = 7.0×10^{-2} M; [indicator] = 2.5×10^{-4} M; temperature = 25.0 °C. Key: (■) **1**; (●) **2**; (◆) **3**. The solid line was calculated on the basis of the mechanisms outlined in eq 6, see Discussion.

to assume that no stable bicarbonate complex is formed because the release of CO_2 was observed during the reaction. In addition, no evidence whatsoever could be found for the presence of such a complex. Therefore, the rate-determining step of the dehydration reaction must be the substitution of the labile water molecule by HCO_3^-, which is a nucleophilic attack on the Cu(II) ion of the model complex.

As has been pointed out, the observed reaction rate is first-order with respect to the total complex concentration C_{com}:

$$V^d = k^d{}_{obs} C_{com} \quad (2)$$

From the following stoichiometric equation (L = ligand)

$$C_{com} = [LCuOH_2^+] + [LCuOH] \quad (3)$$

we have

$$C_{com} = [LCuOH_2^+](1 + K_a/[H^+]) \quad (4)$$

According to the proposed mechanisms

$$V^d = k^d[LCuOH_2^+] = k^d C_{com}[H^+]/([H^+] + K_a) \quad (5)$$

therefore

$$k^d{}_{obs} = k^d[H^+]/([H^+] + K_a) \quad (6)$$

The kinetic data were thus fitted to the suggested mechanisms II and III, for which the corresponding rate law is given in eq 6. Accordingly, a plot of $k^d{}_{obs}{}^{-1}$ versus $[H^+]^{-1}$ should be linear, which is the case for the experimental data (see Figure 5). It is evident from the figure that the catalytic activity decreases with increasing pH and the catalytic activity of the model complexes decreases in the same order, which is consistent with the measurements. This trend suggests that the aqua complex must play a crucial role in the catalyzed dehydration of HCO_3^-, similar to that reported in the literature.[8,17] From fitting the experimental points using eq 6, we can obtain the dehydration rate constant of the rate-determining step k^d, acid dissociation constant K_a, and corresponding pK_a values of the model complexes, which are listed in Table 4.

Table 4. Calculated k^d, K_a, and pK_a Values of the Model Complexes[a]

complex	k^d (s^{-1})	K_a (M)	pK_a
1	0.355	1.61×10^{-8}	7.79
2	0.318	1.77×10^{-8}	7.75
3	0.311	1.86×10^{-8}	7.73

[a] Experimental conditions: $[NaHCO_3] = 7.5 \times 10^{-3}$ M; $[Cu^{2+}] = 1.5 \times 10^{-4}$ M; ionic strength = 0.11 M; [buffer] = 7.0×10^{-2} M; [indicator] = 2.5×10^{-4} M; temperature = 25.0 °C.

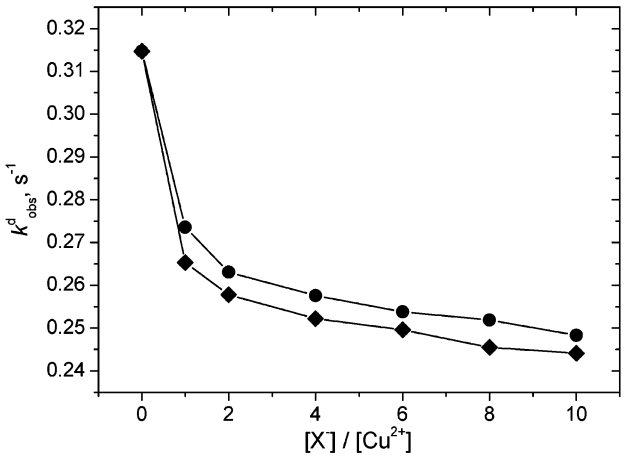

Figure 6. Plot of $k^d{}_{obs}$ versus $[X^-]/[Cu^{2+}]$ for the dehydration of HCO_3^- catalyzed by **1**. Experimental conditions: pH = 7.014; $[NaHCO_3] = 7.5 \times 10^{-3}$ M; $[Cu^{2+}] = 1.5 \times 10^{-4}$ M; ionic strength = 0.11 M; [buffer] = 7.0×10^{-2} M; [indicator] = 2.5×10^{-4} M; temperature = 25.0 °C. Key: (●) $X^- = N_3^-$; (◆) $X^- = NCS^-$.

It is easy to notice in this table that the dehydration rate constants of copper(II) complexes with inhibitors are markedly lower than those without inhibitors. That is, remarkable differences in the dehydration rate constants have been shown between **2**, **3**, and **1**. Meanwhile, noticeable variations of the inhibition effects of NCS^- and N_3^- have been examined. Because the molecular structures of NCS^- and N_3^- are quite similar, we should not expect a significant difference in the inhibition ability between the model complexes with NCS^- and N_3^-. Therefore, a theoretical estimation is needed to evaluate the changes of the inhibition effects, which appears in a later part of this paper. The pK_a values are rather close to that found from the pH titrations of the catalyzed dehydration reaction of HCO_3^- when the limited pH range is taken into account and underline the validity of suggested mechanisms. Again, it was checked that the free Cu(II) ions had no effect on the reaction, so that the observed catalytic effect must be due to the model complexes.

Free Inhibitors. To further confirm mechanism III and have a better understanding of the effects of inhibitors on the dehydration reaction, we also measured the dehydration kinetics of HCO_3^- catalyzed by model complex **1** in different $[X^-]/[Cu^{2+}]$ molar ratios (X^- = free inhibitor N_3^-/NCS^-; Cu^{2+} = copper(II) complex). Figure 6 shows the plot of $k^d{}_{obs}$ versus $[X^-]/[Cu^{2+}]$ for the dehydration of HCO_3^- catalyzed by **1**. Seen from the figure, the catalytic activity decreases with increasing molar ratios of $[X^-]/[Cu^{2+}]$ from 0 to 10,

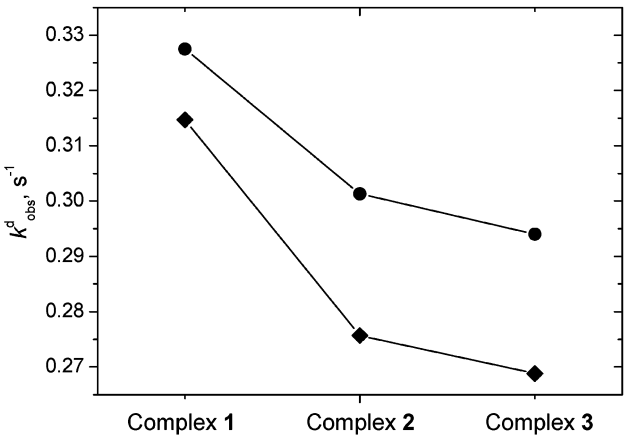

Figure 7. Plot of k^d_{obs} versus the model complexes for the dehydration of HCO_3^- at 298 and 310 K, respectively. Experimental conditions: pH = 7.014; $[NaHCO_3] = 7.5 \times 10^{-3}$ M; $[Cu^{2+}] = 1.5 \times 10^{-4}$ M; ionic strength = 0.11 M; [buffer] = 7.0×10^{-2} M; [indicator] = 2.5×10^{-4} M. Key: (●) 310 K; (◆) 298 K.

Scheme 4

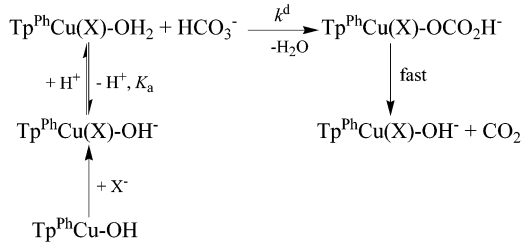

and the inhibition ability of the inhibitor decreases in the order $NCS^- > N_3^-$. What should be mentioned is that, in the case of $[X^-]/[Cu^{2+}] = 1$, k^d_{obs} values observed here are almost the same as those of **2** and **3**, respectively, at the same pH as shown in Figure 5. When the molar ratios of $[X^-]/[Cu^{2+}] > 1$, no marked change in k^d_{obs} is observed. The results here indicate that before the dehydration of HCO_3^- catalyzed by model complex **1** the free inhibitor coordinates to the Cu(II) ion forming a five-coordinated inhibitor adduct, and the remaining uncoordinated inhibitors have little effect on the dehydration reaction. On the basis of these analyses, we present mechanism IV interpreting the effects of free inhibitors on the dehydration of HCO_3^- catalyzed by model complex **1** (Scheme 4). It is easy to note that the catalytic process outlined in mechanism IV is in connection with mechanism III, the five-coordinated aqua model complex being the reactive catalytic species in both mechanisms.

Temperature. The activation parameters for the dehydration reaction were determined from the temperature dependence of the k^d_{obs} values. The temperature-dependent dehydration reaction rate constants are measured at 298 and 310 K, respectively. A plot of k^d_{obs} versus different model complexes for the catalyzed dehydration of HCO_3^- at 298 and 310 K, respectively, is shown in Figure 7. The measurement results show that the k^d_{obs} values increase with increasing reaction temperature, which is consistent with the enzyme catalytic behavior. From the Eyring equation, eq 7,

Table 5. Activation Parameters $\Delta H^{\ddagger}_m$ (kJ mol^{-1}), $\Delta S^{\ddagger}_m$(J K^{-1} mol^{-1}), and E_a (kJ mol^{-1}) of the Rate-Determining Step[a]

model complex	$\Delta H^{\ddagger}_m$	$\Delta S^{\ddagger}_m$	E_a
1	0.108	−326.4	2.476
2	3.151	−317.6	5.678
3	3.179	−317.2	5.706

[a] Experimental conditions: pH = 7.014; $[NaHCO_3] = 7.5 \times 10^{-3}$ M; $[Cu^{2+}] = 1.5 \times 10^{-4}$ M; ionic strength = 0.11 M; [buffer] = 7.0×10^{-2} M; [indicator] = 2.5×10^{-4} M.

and the Arrhenius equation, eq 8

$$\ln(k/T) = -\Delta H^{\ddagger}_m/RT + \Delta S^{\ddagger}_m/R + \ln(R/N_a h) \quad (7)$$

$$\ln(k_2/k_1) = E_a(T_2 - T_1)/RT_1T_2 \quad (8)$$

where the symbols have their usual meaning, the activation parameters of the rate-determining step can be obtained from the corresponding k_d values. The activation enthalpy $\Delta H^{\ddagger}_m$, activation entropy $\Delta S^{\ddagger}_m$, and apparent activation energy E_a are listed in Table 5.

Although the activation parameters are often not discriminating factors in recognizing the reaction pathway, the large negative entropy of activation ($\Delta S^{\ddagger}_m$), however, clearly indicates an associative mode of activation in the rate-determining step. This step can be assigned to the reaction between the aqua model complex and HCO_3^-, which is consistent with our proposed dehydration mechanisms. Again, we should note that the mechanisms proposed in this work are based on the principle that only the aqua complex can react with HCO_3^- in order to catalyze the dehydration reaction. In these cases, it is reasonable to assume that the produced bicarbonate complex is unstable and rapidly releases CO_2. Therefore, the rate-determining step of the dehydration reaction must be the substitution of the labile water molecule by HCO_3^-. The apparent activation energies of model complexes **2** (5.678 kJ mol^{-1}) and **3** (5.706 kJ mol^{-1}) are remarkably higher than that of **1** (2.476 kJ mol^{-1}), which should relate to the variations of activation energy of the rate-determining step. Then, the dehydration reactions, in the presence of inhibitors, are spatially disadvantaged leading to higher activation energy barriers, this being the origin of inhibition that the dehydration reaction of HCO_3^- catalyzed by the model complex is inhibited by inhibitors.

Mechanistic Insight from the Effects of Inhibitors. The catalytic activity of the model complexes in our kinetic measurements is characterized by the pK_a value of 7.9, and therefore, the model complexes exhibit a catalytic activity for the dehydration of HCO_3^- at pH < 7.9. It is easy to note that our proposed mechanism II is well in agreement with mechanism I, the so-called zinc−hydroxide mechanism for CA. The reactive catalytic species in both mechanisms I and II show a tetrahedral geometry of the Cu(II) ion with a N_3O donor set.

In general, mechanisms II and III are quite similar; that is, the dehydration processes of HCO_3^- catalyzed by the model complexes in the absence and presence of inhibitors are comparable with each other. Therefore, the overall mechanism of the dehydration of HCO_3^- catalyzed by the

model complexes can be stated as follows: in the case of pH < pK_a, the aqua model complex exhibits the catalytic activity on the dehydration of HCO_3^- in which the rate-determining step is the substitution of the labile water molecule by HCO_3^-, followed by the rapid decarboxylation of the coordinated bicarbonate molecule as found for many model bicarbonate complexes.[8,17] Despite the similar catalytic process outlined in these two mechanisms, a solvent water molecule coordinates to the Cu(II) ions of **2** and **3**, respectively, to complete a five-coordinated aqua model complex showing a trigonal bipyramidal coordination geometry. This five-coordinated inhibitor adduct is considered the reactive catalytic species in the dehydration of HCO_3^-, which is also confirmed by mechanism IV. It is evident from the latter two mechanisms that the inhibitor is not indeed involved in the catalytic process. However, remarkable inhibition was observed such that k^d_{obs} values of model complexes **2** and **3** are significantly smaller than that of **1**. That is, dehydration of HCO_3^- catalyzed by the model complexes with inhibitors leads to higher activation energy barriers, as verified by the kinetic measurements. The higher activation energy must be the origin of inhibition such that the dehydration reaction catalyzed by the model complexes is inhibited by N_3^- and NCS^-.

Theoretical Calculations of the Effective Atomic Charges. It is evident from the described experimental measurements that the inhibition ability of NCS^- is stronger than that of N_3^-. During the dehydration process of HCO_3^-, the nucleophilic attack of the free HCO_3^- on the Cu(II) ion of the model complex is affected by the effective atomic charge of the Cu(II) ion. In this case, the nitrogen atom of the inhibitor (N_3^-/NCS^-) that coordinates to the Cu(II) ion serves as the electron donor. Low effective atomic charges caused by stronger donor inhibitors are disadvantageous to the nucleophilic attack of the free HCO_3^- ion on the Cu(II) ion. To obtain more information on the variations in the effective atomic charge of the Cu(II) ion by coordinating different inhibitors (N_3^-/NCS^-), we have carried out theoretical calculations of **2** and **3** at the UHF level, using a lanl2dz basis set for the Cu atoms and the corresponding basis set for each of the other atoms. Because the Mulliken population analysis is very dependent on the basis set used, an NBO population analysis has been performed, which works better in these cases. On the basis of the crystal data available in the work, the effective atomic charges of the Cu(II) ion can be obtained quantitatively by these calculations. The values have been found to be 0.928 and 0.890 for the Cu(II) ions of **2** and **3**, respectively. Therefore, we can conclude that the electrons from the N donor atom of the inhibitor NCS^- are more delocalized on the Cu(II) ion leading to the decrease of the effective atomic charge of the Cu(II) ion, which can rationalize the variations in inhibition ability between two inhibitors, N_3^- and NCS^-.

4. Conclusions

In summary, we have performed here the detailed kinetic study of the dehydration of HCO_3^- catalyzed by a series of half-sandwich copper(II) complexes [Tp^{Ph}]CuX. The apparent dehydration rate constant k^d_{obs} of **2** and **3** is markedly lower than that of **1**, as shown in four aspects (concentration of the model complexes, pH value, free inhibitors, and temperature): (1) The apparent dehydration rate constant k^d_{obs} varies linearly with total Cu(II) concentration, and the catalytic activity of the model complexes decreases in the order **1** > **2** > **3**. (2) The catalytic activity decreases with increasing pH indicating that the aqua model complex must be the reactive catalytic species in the catalyzed dehydration reaction and the rate-determining step is the substitution of the labile water molecule by HCO_3^-. The coordination atmospheres of the aqua model complexes in the absence and presence of inhibitors are four-coordinated tetrahedron and five-coordinated trigonal bipyramid, respectively. (3) The free inhibitor coordinates to the Cu(II) ion of **1** forming a five-coordinated inhibitor adduct before the dehydration of HCO_3^- is catalyzed by model complex **1**, and the remaining uncoordinated inhibitors have little effect on the dehydration reaction. (4) The k^d_{obs} values increase with increasing reaction temperature, and the apparent activation energies of the model complexes with inhibitors are remarkably higher than that of the model complex without inhibitors. The large negative entropy of activation indicates an associative mode of activation in the rate-determining step.

In all, the dehydration reaction of HCO_3^- catalyzed by the model complexes is inhibited by inhibitors, which leads to a higher activation barrier being the origin of inhibition. In particular, the inhibition ability of the inhibitor NCS^- is stronger than that of the inhibitor N_3^-, which can be rationalized by the decrease in effective atomic charges of the Cu(II) ions as revealed by the theoretical calculations in this work.

Acknowledgment. This work was supported by the NSFC (29971017, 90101028) and the TRAPOYT of MOE, China.

Supporting Information Available: Full lists of the crystallographic data for **3**. This material is available free of charge via the Internet at http://pubs.acs.org.

IC025926H